

We previously measured from $\rho(\tau, \xi)$, $V' = 60 \pm 4$ cm/sec and $V = 46 \pm 4$ cm/sec. The agreement between V' and V_1 and between V and V_2 is clearly within the accuracy of the experiment. The error estimates are intended to indicate only the size of the random errors resulting from a finite number of samples. We would expect $V_{\{\Delta\phi\}-s}$, the velocity measured from the $\{\Delta\phi\}$ versus s plot, to be equal to V_1 if the distribution of cross-spectral amplitude were symmetric in $\Delta\phi$. The distribution is not symmetric and the difference between $V_{\{\Delta\phi\}-s}$ and V_1 is the difference between the mean and the point of maximum of the distribution.

Additional work is clearly required to properly evaluate this technique. At the moment, however, it appears to be a very promising method for measuring the true drift velocity V with data from only two fixed probes separated along the direction of motion.

The observations described in this report are for simple turbulence without the presence of dispersive wave phenomena. The Doppler shift effect, which distorts the simple $\{\Delta\phi\}$ versus s velocity measurement for the turbulence case will not apply to linearly superimposed waves. The $\{\Delta\phi\}$ versus s plot for dispersive waves will usually not be a straight line but will display some curvature from which the dispersion relation for the waves might be scaled. Such a measurement would be very valuable in an ionosphere or solar wind scintillation experiment. However, even if the observer knows that he is measuring a cross-spectrum resulting only from wave effects, cross-spectral analysis gives unambiguous measurements of velocity and dispersion only for restricted geometries.

An attempt to make such measurements with ionospheric scintillations has recently been reported by Briggs and Golley (14). They conclude that the apparent dispersive effect which they measure was probably due to structure moving with different velocities at different altitudes rather than to true dispersive wave modes.

Similarly, if a wave structure which is generating scintillations is not all propagating in the same direction, but exists as an angular spectrum of waves, the cross-spectral results will be confused. The scintillation measurement will respond only to the projection of the wave lengths and velocities of the diffracting wave structure on a plane normal to the direction of the probing ray. The resulting cross-spectrum may

assume very rich structure which need not be uniquely related to the diffracting screen geometry.

When turbulence and dispersive wave phenomena are combined, as they probably are in the solar wind, the situation becomes even more complicated. It may prove possible to scale a dispersion relation from the $\Delta\phi$ versus s cross-spectral distribution surface in some cases. We find that when used in scintillation studies cross-correlation and cross-spectral measurements will yield unambiguous information about the diffracting screen only when the observer can safely make additional assumptions about the screen structure.

While these results demonstrate certain limitations of the cross-correlation and cross-spectrum analysis methods, they do not express a fundamental limit to the amount of information available about the irregular structure from diffraction measurements. It may be possible to obtain additional information with techniques of higher-order spectral analysis (15). Further, it is often true that special characteristics of the medium under study allow logical resolution of the ambiguities limiting the diffraction techniques. For example, plasma resonances may be expected in the ionospheric or interplanetary plasmas, and these resonances should often be useful in the experimental interpretations.

M. GRANGER MORGAN
KENNETH L. BOWLES

Department of Applied Electrophysics,
University of California at San Diego,
La Jolla 92037

References and Notes

1. See, for example, A. Hewish, P. A. Densison, J. D. H. Pilkington, *Nature* **209**, 1188 (1966); P. A. Densison and A. Hewish, *ibid.* **213**, 343 (1967).
2. See, for example, M. H. Cohen, E. J. Gundermann, H. E. Hardebeck, L. E. Sharp, *Astrophys. J.* **147**, 449 (1967); M. H. Cohen, E. J. Gundermann, D. E. Harris, *ibid.* **150**, 767 (1967).
3. K. Bartusek and D. G. Felgate, *Australian J. Phys.* **19**, 545 (1966).
4. G. R. Ochs, paper presented to the 1967 Fall URSI meeting at Palo Alto, California (U.S. National Meeting of the International Scientific Radio Union).
5. B. H. Briggs, G. J. Phillips, D. H. Shinn, *Proc. Roy. Soc. London Ser. B* **63**, 106 (1950).
6. L. C. Fedor, *J. Geophys. Res.* **72**, 5401 (1967).
7. E. E. Gossard, *ibid.*, p. 1563.
8. A. Favre, J. Gaviglio, R. Dumas, *Phys. Fluids Suppl.* **S138** (1967).
9. W. W. Willmarth and C. E. Wooldridge, *J. Fluid Mech.* **14**, 187 (1962).
10. M. J. Fisher and P. O. A. L. Davies, *ibid.* **18**, 97 (1963).
11. J. A. B. Wills, *Proc. Intern. Congr. Appl. Mech. 11th Munich*, p. 889 (1964). [See also *J. Fluid Mech.* **20**, 417 (1964).]
12. The line for fixed time delay and variable probe separation may be hard to draw with accuracy. An equivalent way of deducing V is to construct the envelope of the cross-correlation curves $\rho(\tau, \xi_0)$. This envelope will be the moving frame auto-correlation. The points where the moving frame auto-correlation is tangent to the cross-correlation curves can be scaled as τ_n . If ξ_n are the corresponding probe separations then $V = \xi_n/\tau_n$.
13. J. L. Lumley, *Phys. Fluids* **8**, 1056 (1965).
14. B. H. Briggs and M. G. Golley, paper presented to the IAGA/URSI symposium Upper Atmosphere Winds, Waves, and Ionospheric Drifts, St. Gallen, Switzerland, October 1967.
15. See, for example, K. Hasselmann, W. Munk, G. MacDonald, "Bispectra of Ocean Waves," in *Time Series Analysis*, M. Rosenblatt, Ed. (Wiley, New York, 1963); T. Madden, "Spectral, cross-spectral, and bispectral analysis of low frequency electromagnetic data," in *Natural Electromagnetic Phenomena Below 30 kc/s*, D. F. Bleil, Ed. (Plenum, New York, 1964); M. P. Aubry, *Ann. Astrophys.* **29**, 389 (1966) and **30**, 101 (1967).
16. We thank R. D. Abney, C. W. Van Atta, M. H. Cohen, W. A. Coles, and C. H. Gibson for their helpful suggestions and discussions. The work was supported partially by NASA grant NsG-538, partially by Project DEFENDER 67/68-181, and partially by NSF grant GA-744.

20 June 1968

Murray Fracture Zone: Westward Extension

Abstract. *The Murray Fracture Zone is one of the principal east-west rifts in the crust of the northeast Pacific basin. As judged by bathymetric and magnetic surveys, the Murray approaches the Hawaiian Archipelago as a well-defined zone of ridges and troughs accompanied by strong, linear magnetic anomalies. It loses its topographic expression on encountering the Hawaiian Arch but can be traced magnetically to its intersection with the Hawaiian Ridge in the vicinity of Laysan Island (near 172°W). All evidence tends to discount a previously suggested genetic relation between the Murray Fracture Zone and the Necker Ridge.*

The long, linear fracture zones (1), which trend in an east-west direction across the northeast Pacific basin and offset well-defined patterns of north-south trending magnetic anomalies, are of primary significance and must be considered in any geological model of the earth. One of these, the Murray Fracture Zone, lies between and parallels two others, the Mendocino and the

Molokai fracture zones. The Murray Fracture Zone has been traced from a point off the coast of southern California westward for more than 4000 km. It has been suggested (2, 3) that before reaching the Hawaiian Archipelago, the Murray bends abruptly southwestward and continues into the Necker Ridge which trends southwestward from Necker Island (Fig. 1). De-

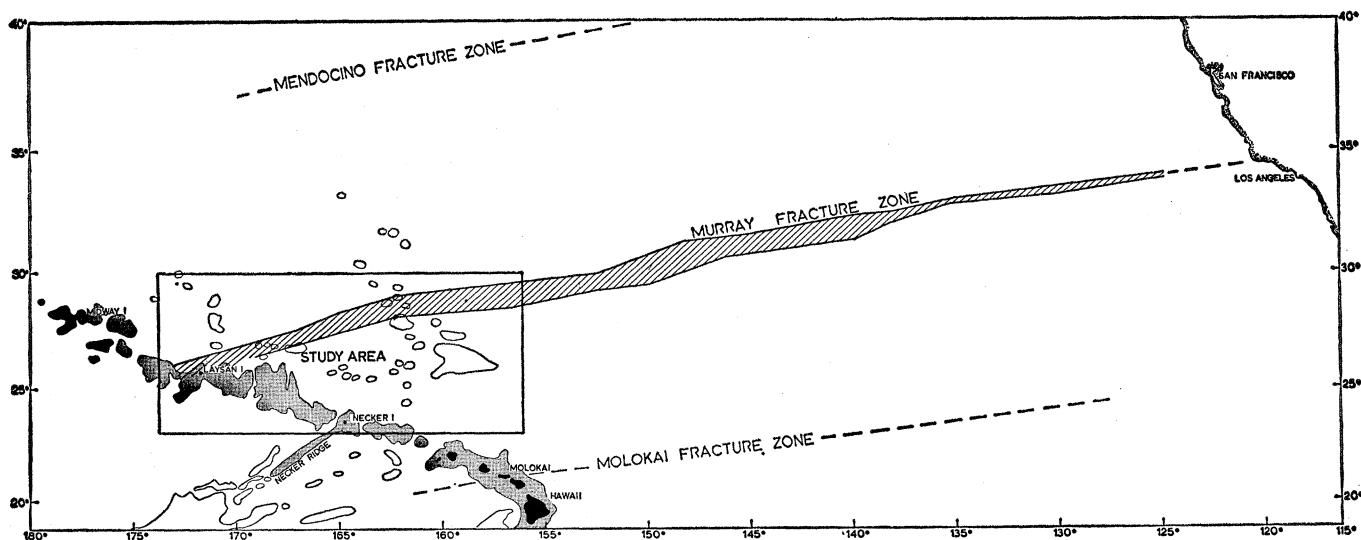


Fig. 1. Murray Fracture Zone and the Hawaiian Ridge. The ridge (stippled areas) and other topographic features (limited to the Hawaiian area) are defined by 3700 m contours (from U.S. Coast and Geodetic Survey chart 9000). Bathymetric and magnetic trends within the outlined area are shown in Fig. 2.

tailed bathymetric and magnetic data (4), however, indicate that the Murray passes well north of Necker Island and intersects the Hawaiian Ridge near Laysan Island (Fig. 2).

The Murray Fracture Zone approaches the Hawaiian structure (west of 157°W) as a well-defined bathymetric feature (Figs. 1 and 2a). It occurs as a band of parallel asymmetrical ridges and troughs trending generally west-southwest. Between 157°W and 161°W it has a ridge-to-trough relief on the order of 1000 m, with a maximum depth of 6520 m occurring at about 158°W in one of the troughs. Bathymetric profiles of the Murray Fracture Zone in this region are almost identical to one at $152^{\circ}30'\text{W}$ which Menard (1, fig. 3.3) presents as a typical example of the double-asymmetrical-ridge type of fracture zone. The topography is accompanied throughout by a wide band of linear magnetic anomalies characterized by strong positive magnetic lineations along the northern margin (Fig. 2b). At about $161^{\circ}30'\text{W}$ the Murray Fracture Zone encounters and is masked for about 130 km by the northwest trending Musicians Seamount Province. The northern limit of the Hawaiian Arch also lies within this region (5). Thus three structural features intersect at approximately the same location ($28^{\circ}30'\text{N}$ and 162°W). Several changes take place in the Murray Fracture Zone as it passes westward across this intersection: (i) it loses about half of its vertical relief, (ii) its trend changes about 5° toward the south, and (iii) it acquires a strong negative magnetic lineation along its southern margin. Its general morpho-

logical character is retained, and it continues as a well-defined zone to 165°W before entering a region for which detailed data are lacking.

Data coverage resumes west of $167^{\circ}30'\text{W}$, but here the Murray has lost its bathymetric expression completely. The characteristic magnetic lineations show that the Murray Fracture Zone continues across the relatively smooth Hawaiian Arch and that it intersects the Hawaiian Ridge in the vicinity of Laysan Island. Between $167^{\circ}30'\text{W}$ and $170^{\circ}30'\text{W}$ the trend is represented by a pair of large magnetic lineations which are offset or rotated at the crest of the arch where several large seamounts are located. At this same location two large anomalies branch off the main trend of the Murray, extend northwesterly for about 130 km, and die out before reaching an elongate dipole anomaly perpendicular to them. These anomalies have no bathymetric expression—a suggestion that they result from deep-seated intrusives whose surface expression has been covered and smoothed by materials forming the Hawaiian archipelagic apron (6). The various features may reflect the intersection of the Murray Fracture Zone with a zone of tension along the crest of the arch. A decrease in the intensity of the anomalies, and discontinuities in the individual lineations, occur where they encounter the Hawaiian Deep which is unusually well developed along the general trend of the lineations.

The observed bathymetric and magnetic relations along the Murray Fracture Zone are similar to those associated

with the Molokai Fracture Zone as it intersects the Hawaiian Ridge farther south near the island of Molokai. Malahoff *et al.* (3) show that the Molokai Fracture Zone loses its bathymetric expression as it encounters the Hawaiian Deep but can be traced magnetically across the Ridge and westward for several hundred miles.

According to Malahoff *et al.* (7), most magnetic anomalies in the Hawaiian area can be divided into two groups: (i) local dipole anomalies related to centers of volcanism and (ii) elongate dipole anomalies related to dike complexes and crustal rift zones. Both types of magnetic expression are apparent in Fig. 2b. Local dipole anomalies are shown by relatively short, parallel pairs of positive and negative lineations, randomly oriented around a general east-west trend. As Malahoff *et al.* found to the east (7), most dipoles in this area exhibit normal polarization (positive anomaly to the south) with respect to the present magnetic field of the earth and in almost all cases are associated with pronounced topographic features. Several large east-west ridges located near 160°W have elongate anomalies associated with them, but only locally do their single-peak values exceed 200 gammas (shown by heavy lines) ($1 \text{ gamma} = 10^{-5}$ oersted). Hence, the anomalies appear due to topographic effects (near-surface volcanism) rather than deep-seated intrusives along a major rift zone. The second group of magnetic anomalies are long and linear, do not necessarily have topographic expression, generally trend in one of two major directions, and in

places maintain high amplitudes over great distances. These may be caused by deep-seated intrusives along primary rift zones. One trend is associated with the Murray Fracture Zone and closely parallels the ridge and trough topography of the Murray east of 165°W, while west of 167°30'W, where there is no bathymetric expression, the "rift zone" magnetic anomalies clearly continue the trend across the crest of the arch. The other principal trend suggestive of primary fracturing is shown by a series of east-west lineations along portions of the ridge. These elongate anomalies have little correlation with local topography and closely parallel regional trends of the ridge.

An east-west interruption of the general northwest trend of the Hawaiian

Ridge occurs near 169°W (Fig. 1). This configuration could be explained by left-lateral displacement of the ridge along the Murray Fracture Zone; however, large right-lateral displacements are indicated along the eastern portion of the Murray (8), and evidence suggests that these displacements increase westward. A more plausible explanation of this east-west deviation in trend is that the Murray Fracture Zone is older and, as a zone of weakness, influenced formation of this portion of the ridge.

The topographic lineations which continue the trend of the Necker Ridge northeast of Necker Island do not appear to be related to primary fracturing. This conclusion is based on the lack of high-amplitude elongate magnetic anomalies within this zone and

also on the fact that the bathymetric trends, although somewhat subtle, are more pronounced than those of the magnetics, a relation opposite to that generally observed along zones of primary rifting.

Several cross-cutting bathymetric and magnetic structures trending northeast occur within the Murray Fracture Zone between 156°W and 160°W, and also the Murray appears to be slightly offset, left laterally along a similar trend, between 148°W and 152°W (Fig. 1). These subtle relations may be connected to the similar trending bathymetric lineations associated with the Necker Ridge. If so, this would indicate that these structures postdate the Murray Fracture Zone.

Bathymetric charts of the region west

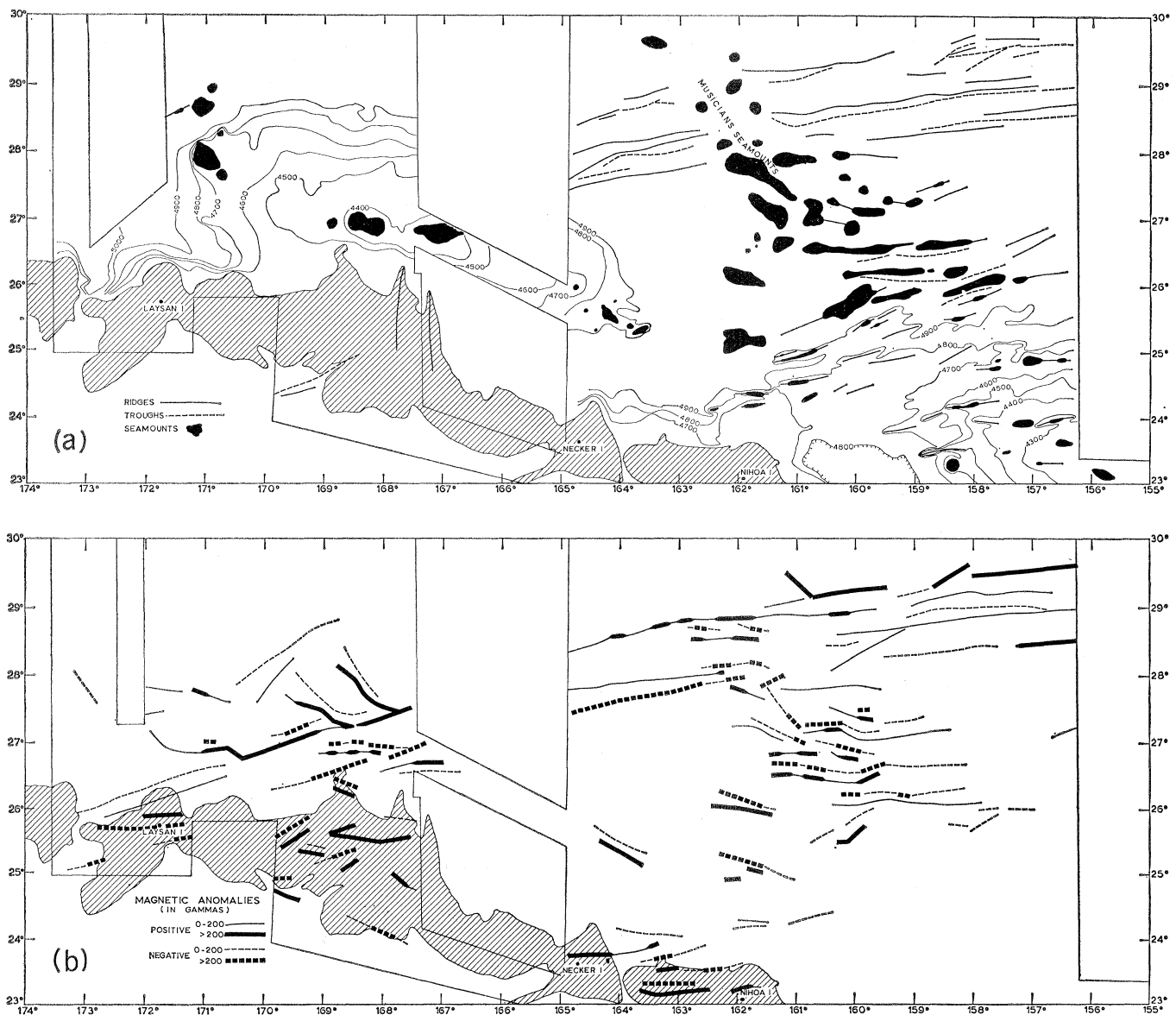


Fig. 2. Bathymetric trends (a) and magnetic trends (b) along the Murray Fracture Zone north of the Hawaiian Islands. Areas shoaler than 400 m are shown in black for seamounts (a) and are hachured over the Hawaiian Ridge (a and b). Selected contours are used to show the location of the Hawaiian Arch and Deep (a). Outlined areas indicate regions for which there is no detailed data.

of the ridge (9) show several lineations in the form of strings of abyssal hills (ridges?) and regional offsets in bathymetry, which conform in trend and general position to an extension of the Murray Fracture Zone.

FREDERIC P. NAUGLER
BARRETT H. ERICKSON

*Pacific Oceanographic Research
Laboratory, Environmental
Science Services Administration,
Seattle, Washington 98102*

References and Notes

1. H. W. Menard, *Marine Geology of the Pacific* (McGraw-Hill, New York, 1964), p. 260.
2. G. P. Woollard, in *Continental Margins and Island Arcs*, W. H. Poole, Ed. (Geological Survey of Canada Paper 66-15, 1965), p. 296.
3. A. Malahoff, W. E. Strange, G. P. Woollard, *Science* **153**, 521 (1966).
4. These data were collected by the U.S. Coast and Geodetic Survey ships *Pioneer* and *Surveyor* during project SEAMAP. For brief résumé of the USC&GS SEAMAP survey, see T. V. Ryan and P. J. Grim, "A new technique for correcting echo soundings," *Intern. Hydrograph. Rev.*, in press.
5. F. Naugler and T. V. Ryan, ESSA Research Laboratories technical report, Boulder, Colo., in preparation.
6. H. W. Menard, *Bull. Geol. Soc. Amer.* **40**, 2195 (1956).
7. A. Malahoff, W. E. Strange, G. P. Woollard, *Pac. Sci.* **20**, 265 (1966).
8. A. D. Raff, *J. Geophys. Res.* **67**, 417 (1962).
9. G. V. Udintsev, Ed., *General Bathymetric Map of the Ocean: Pacific Ocean* (Department of Geodetic Cartography, Geology Commission, Moscow, 1964).

28 June 1968

Diosgenin and β -Sitosterol: Isolation from *Solanum* *Xanthocarpum* Tissue Cultures

Abstract. *Diosgenin and β -sitosterol were isolated from *Solanum xanthocarpum* callus, crystallized, and chemically characterized. That these metabolites, particularly diosgenin, form in significant amounts in tissue culture may prove useful.*

Formation, in tissue culture, of nicotine in *Nicotiana* (1), tropane alkaloids in *Datura* (2), substances similar to digitalis glycosides in *Digitalis* (3), vinca alkaloids in *Catharanthus* (4), reserpine in *Alstonia* (5), indole alkaloids in *Ipomoea* (6), visnagin in *Ammi* (7), formononetin in *Cicer* (8), and solasonine in *Solanum* (9) has been observed.

Steroids occur in solanaceous plants, and a few have been extracted from tissue cultures of *Nicotiana* (10). We now report on the isolation and identification of β -sitosterol and diosgenin from callus tissues of *Solanum xanthocarpum* (Solanaceae). Actively proliferating calli raised from the aseptic culture of young

defoliated shoots on Murashige and Skoog's basal medium fortified with growth supplements (11) were used.

β -Sitosterol was isolated as follows. A portion (25 g) of oven-dried (60°C for 48 hours) callus was powdered and extracted in a Soxhlet apparatus with chloroform for 24 hours. The extract was concentrated to dryness and chromatographed on a column (1 by 10 cm) of silica gel (< 0.08 mm, E. Merck); the column was eluted with a benzene-ethyl acetate gradient. Fractions containing the steroid component were pooled and purified by thin-layer chromatography (silica gel G, E. Merck) with the following solvent systems: benzene and ethyl acetate (85:15); and chloroform and ethyl acetate (95:5). Fifteen milligrams of a homogeneous product was obtained and purified by crystallization from methanol (plates, 10 mg; m.p. 137°C). Elemental analysis showed 83.8 percent of carbon and 12.2 percent of hydrogen. The formula $C_{29}H_{50}$ requires 84.0 percent of carbon and 12.2 percent of hydrogen. The color reactions with $SbCl_3$ and concentrated H_2SO_4 indicated that the compound was a 3- β -hydroxy- Δ^5 -steroid; this structure was confirmed by a positive Liebermann test.

The infrared (IR) spectrum of this product was superimposable with that of β -sitosterol. An acetyl derivative of the compound was prepared with acetic anhydride and pyridine. On crystallization from methanol, it melted at 126°C. No depression was observed in the melting point of the parent compound or its acetate on admixture respectively with authentic β -sitosterol or its acetate, thereby providing conclusive proof of the formation of β -sitosterol as a major product in tissue cultures of *S. xanthocarpum*.

Diosgenin was isolated as follows. The residue after the chloroform extraction was extracted with 95 percent ethyl alcohol in a Soxhlet apparatus. The solvent was removed, the residue was hydrolyzed (3 percent HCl for 3 hours), and the hydrolyzate was extracted with chloroform (4 by 25 ml) after neutralization with ammonia. The concentrated extract was chromatographed on silica gel column (< 0.08 mm, E. Merck) with chloroform and ethyl acetate mixtures. The fractions that gave positive $SbCl_3$ and concentrated H_2SO_4 color tests were combined and further purified by thin-layer chromatography on silica gel G with chloroform, and chloroform-ethyl acetate (95:5). The IR spectrum of the crys-

Table 1. Steroid content from berries and tissue cultures of *Solanum xanthocarpum*.

| Source | β -Sitosterol (%) | Diosgenin (%) |
|-----------------|-------------------------|---------------|
| Berries | 0.017 | 0.001 |
| Tissue cultures | .04 | .008 |

talline product (2 mg) was superimposable with that of authentic diosgenin, thus establishing the identity of the compound. On a thin-layer plate its behavior was like that of the reference sample. The acetyl derivative of the product showed the same R_F value as that of diosgenin acetate, further confirming the isolated compound as diosgenin.

Chemical examination of *S. xanthocarpum* berries also resulted in the isolation of diosgenin, a compound already reported from the species (12). But the predominant constituent was β -sitosterol, known to occur in the related species *S. khasianum* (13). The steroidal content from tissue cultures as compared with the berries is given in Table 1.

Although only trace amounts of the steroidal alkaloid solasonine were detected earlier (9), the tissue cultures of *S. xanthocarpum* have yielded β -sitosterol and diosgenin in quantities much higher than that obtained from the growing plant.

M. R. HEBLE
S. NARAYANASWAMI
M. S. CHADHA

*Biology Division, Bhabha Atomic
Research Centre, Bombay-74, India*

References

1. T. Speake, P. McClosky, W. K. Smith, T. A. Scott, H. Hussey, *Nature* **201**, 614 (1964); T. Furuya, H. Kojima, K. Syono, *Chem. Pharm. Bull. (Tokyo)* **14**, 1189 (1966).
2. W.-N. Chan and E. J. Staba, *Lloydia* **28**, 55 (1965).
3. S. A. Büchner and E. J. Staba, *J. Pharm. Pharmacol.* **16**, 733 (1964).
4. L. A. Harris, H. B. Nylund, D. P. Carew, *Lloydia* **27**, 322 (1964); G. B. Boder, M. Gorman, S. Johnson, P. J. Simpson, *ibid.*, p. 328; I. K. Richter, K. Stolle, D. Groger, M. Mothes, *Naturwissenschaften* **52**, 305 (1965).
5. D. P. Carew, *Nature* **207**, 89 (1965).
6. E. J. Staba and P. Laursen, *J. Pharm. Sci.* **55**, 1099 (1966).
7. B. Kaul and E. J. Staba, *Science* **150**, 1731 (1965).
8. B. M. Sayagaver, N. B. Mulchandani, S. Narayanaswami, *Lloydia*, in press.
9. M. R. Heble, S. Narayanaswami, M. S. Chadha, *Naturwissenschaften* **55**, 350 (1968).
10. P. Benveniste, L. Hirth, G. Ourisson, *Phytochemistry* **5**, 31 (1966); T. Furuya, H. Kojima, K. Syono, *Chem. Pharm. Bull. (Tokyo)* **15**, 901 (1967).
11. P. S. Hao and S. Narayanaswami, *Planta* **81**, 372 (1968).
12. Y. Sato and H. G. Latham, Jr., *J. Amer. Chem. Soc.* **75**, 6067 (1953).
13. P. C. Maiti, S. Mookerjee, R. Mathew, *J. Pharm. Sci.* **54**, 1828 (1965).

17 July 1968